Flow visualization in a laboratory vaned diffuser

R. B. Brownell, R. D. Flack, M. C. Davis† and J. G. Rice*

An experimental model of a vaned diffuser with rectangular flow cross-sections was constructed of clear plastic for flow visualization studies. A swirl generator was used to induce fluid rotation without subjecting the diffuser to any unsteady and irregular impeller flow phenomena. The blades were of a thin circular arc shape. The clear plastic construction allowed large-scale flow visualization with tufts attached to the diffuser wall and dye injected into the separation regions. Four conditions were tested: a vaneless, a four-vaned, a six-vaned, and an eight-vaned diffuser. Each test was conducted at an average Reynolds number of 20 000, based on passage thickness. In the absence of diffuser blades the flow angle was not radially constant, as a result of the viscous effects, varying as much as 11° from the ideal 16°. With four blades installed, separation began at 23% of the blade length from the leading tip. At the peak development of the separation regions 34% of the flow area was blocked. Separation began at 27% from the leading edge when six blades were used. Finally, with eight blades in place, separation began at 50% of the blade length from the leading tip; at the peak development of the separation regions 64% of the flow area was blocked.

Keywords: *diffuser flow, separated flow, vaned flow, flow visualization*

Introduction

The purpose of a diffuser in a turbomachine is to convert to static pressure a portion of the kinetic energy possessed by the fluid exiting the impeller. Ideally, a diffuser provides efficient pressure recovery over a wide range of flow conditions, but realistically this is rarely possible. Two diffuser types are in common usuage today: the vaneless and the vaned diffusers.

The vaneless diffuser is a simple annular region, usually of approximately constant width, that surrounds the impeller. The radial velocity component of the diffuser flow is reduced by area increase, and the tangential velocity component is reduced by the requirement of constant fluid angular momentum. A vaneless diffuser can offer a wide range of operating conditions, but if it is to achieve substantial pressure recovery it tends to be bulky.

A vaned diffuser uses blades to guide the flow to obtain a higher rate of diffusion than is possible with a vaneless diffuser, and a number of different blade designs have been used successfully. The operating range of the vaned diffuser is, however, typically less than that of the vaneless diffuser because separation from the blades causes substantial passage blockage at off-design flow conditions. Additional complications can be introduced into the system by rotating impeller wakes or by interaction between the impeller and diffuser. Despite the complexities, the vaned diffuser can usually provide a higher peak efficiency and less bulk than its vaneless counterpart.

Until recently, pump designs were based on previous, successful machines and limited empirical data. Numerical methods for calculating flow characteristics are currently under development, which could be used by the designer to estimate the performance of a given system before it is manufactured. These theoretical models must first be compared with experimental data to verify their predictive value, however.

A substantial portion of turbomachinery flow research has dealt with the impeller. Fewer works have investigated the important interaction between the impeller and the subsequent diffusing elements. Vaneless diffusers or volutes were typically used in these experiments because they exhibit an apparently simple two-dimensional unobstructed flow geometry. A review of literature on vaneless diffusers and volutes is included in Ref 1 and others. In summary, much of the vaneless diffuser research has been performed to provide an understanding of the dissipation of impeller jet/wake flows. Several viable analyses have been produced to predict the losses caused by this rotating wake phenomenon. Intensive research focusing on vaned diffuser flow behaviour is only beginning to be published, although the importance of this information has been recognized for nearly half a century. For the sake of brevity, only experimental research on vaned diffusers is reviewed below.

Pampreen[2] studied the operating characteristics of different cascade diffusers. Various blade shpaes and positions were tested for their efficiency and pressure ratio. He found that a cascade diffuser could perform better than a conventional diffuser for identical inlet and exit conditions, with less loss and a larger stall-free range.

Sakurai[3] studied flows within a single diffusing passage with circular arc blades without the influence of impeller-generated flow irregularities or diffuser blade tip effects. Pressures were measured along the walls of a logarithmic spiral passage. A theoretical analysis based on boundary layer development complemented the experiment. He concluded that within the limitations of separation, efficiency increased with the increase of area ratio.

Baghdadi[4] experimentally examined the flows in a vaned diffuser in an industrial compressor and developed a vortex rig to study the steady flows in a similar diffuser. By comparing results from the two rigs the author found that the unsteady flows in the compressor did not adversely affect the diffuser performance.

Yoshinaga *et al*[5] tested sixteen different vaned diffusers in a model compressor using pressure measurements to determine the overall behaviour of the diffuser flows. Little discussion on the geometry and performance of individual diffusers was included; instead the authors suggested various general design criteria for improving compressor performance. The authors indicated that the leading edge shape of the vanes has considerable influence on the diffuser performance.

Krain[6] used a laser velocimeter to accurately measure velocities in an experimental compressor at the impeller exit. Velocity measurements were made separately with a vaneless and with a wedge-shaped vaned diffuser installed in the compressor. Comparison indicated that the vaned diffuser had only a weak influence on the impeller exit velocity profile.

Senoo, Hayami and Ueki[7] theoretically and experimentally

† Digital Inc, Andover, MA, USA
* Department of Mechanical and Aerospace Engineering, University of Virginia, Charlottesville, VA 22901, USA

0142-727X/87/010037-07$3.00

examined the effect of cascading two airfoil-type diffuser blades. The front row was designed for low flow rates while the back row was designed for high flow rates. The authors experimentally found that the tandem-cascade diffuser possessed a wide range of stable operation and produced better pressure recovery than a similar vaneless diffuser. Good agreement was found between predicted and measured performance.

Bammert, Jansen and Rautenberg[8] examined the performance of three vaned diffuser designs—cambered vane, straight channel, and twisted vane—within a test compressor rig. The three diffusers had the same design point but were geometrically dissimilar. Pressure and temperature measurements indicated that the twisted blade diffuser generally produced the highest efficiencies and pressure ratios.

Stein and Rautenberg[9] measured pressures in two compressor vaned diffusers. In this research the passage width was varied and the authors found the smallest passage most efficient. The 3-D pressure field also indicated where specific improvements for the three-dimensionality of the blades could be made.

In summary, most of the experimental work which has concentrated on vaned diffusers has resulted in empirical performance data. Little attempt has been made to accurately measure or predict the fundamental incompressible flow behaviour within vaned diffusers.

For this research a working model for a laboratory experimental vaned diffuser was developed in which flow visualization and laser velocimetry (LV) could be used. The objective of this paper is to present qualitative flow patterns for this diffuser. The data generated by the rig will be used as benchmark data for numerical method evaluation. A swirl generator instead of an impeller was used to supply flow to the diffuser in order to eliminate the possibility of unsteady impeller flows. Four diffuser configurations were studied: a vaneless diffuser, a four-bladed, a six-bladed, and an eight-bladed vaned diffuser. The blades were of a thin circular arc shape. The flow was in the turbulent regime.

Of particular interest was the identification of the onset and extent of separation of the flow from the diffuser blades. A field of flexible tufts was used to measure the flow angle throughout the diffuser on the side walls. Dye injection was employed to identify more completely the shape of the separation regions. The visualization data presented herein will be useful in evaluating the 2-D numerical viscous flow method in Ref 10 and other numerical models that are currently being developed. Future data will include detailed LV measurements for quantitative evaluation of the performance.

Experimental details

The diffuser model

The diffuser model had three main flow regions: the swirl generator, the actual diffuser test region, and the plenum which collected the discharged flow. Fig 1 shows a cross-sectional view of the diffuser, showing the three regions.

Two 76 mm ID, 279 mm long Plexiglas inlet pipes fed into the centre of the test region, one from each side, allowing observation of the flow before entering the diffuser. The two diffuser walls were made of 12.7 mm Plexiglas and were spaced 12.7 mm apart. They were circular in shape with a diameter of 610 mm. Each of the two inlet pipes was permanently fixed to the centre of each of the plates.

The inlet pipes lead directly to an annular swirl generator or 'non-rotating impeller'. Fig 1 shows how the swirl generator was positioned at the centre of the diffusing region. The swirl generator had a 152 mm OD with a 76 mm ID; it was 12.7 mm wide internally. It contained 32 thin, tapered blades intended to induce a 16° logarithmic spiral flow in the test region.

Multiple slots were cut into the diffuser walls so that four, six, or eight equally spaced blades could be installed as required. Fig 1 depicts an eight-bladed arrangement. The blades were made of 3 mm Plexiglas tapered at both ends and permanently bent to fit their matching slots. For ease of construction the blades were a circular arc shape with a radius of 185 mm, an inlet angle of 16°, and an exit angle of 20°. The leading tip was located at a radius of 135 mm and the trailing tip at a radius of 195 mm. When not in use the blade slots were filled and smoothed flush with silicon caulking compound. Fig 2 defines the flow angle ψ, reference angle θ, and dimensionless radius $\bar{r}$. The values of reference angle θ to the leading edge of the first vane for the four-, six- and eight-vaned configurations were 45°, 30° and 0°, respectively.

Near the periphery of the test region, between the radii of 267 mm and 285 mm, a permanent set of 72 equally spaced baffle guide vanes was installed to help isolate the diffuser flow from any plenum influence. These baffle vanes were of 3 mm straight Plexiglas, tapered at the leading end, and set at a 16° angle to align with the expected ideal flow.

Dye injection holes were installed at 75% of the blade length from the leading tip of the blades. The locations of these holes are shown on Fig 1. The holes were 1.6 mm diameter and were 3 mm from the convex side of the blade.

The plenum had an outside diameter of 812 mm and an internal width of 76 mm. The design of the plenum and its important dimensions are detailed in Fig 1. Twelve 25 mm ID

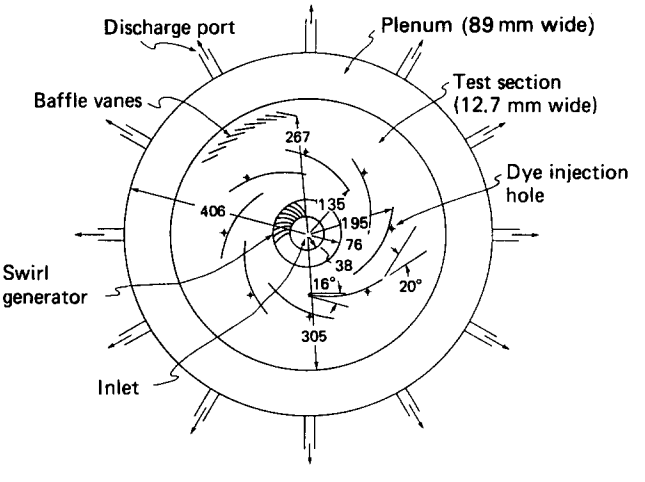

Figure 1 Schematic diagram of diffuser. All dimensions: mm

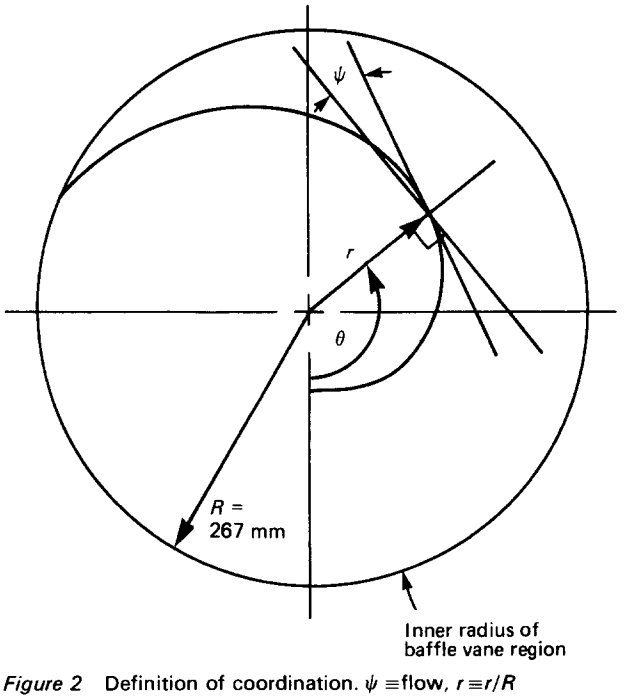

Figure 2 Definition of coordination. $\psi \equiv$flow, $r \equiv r/R$

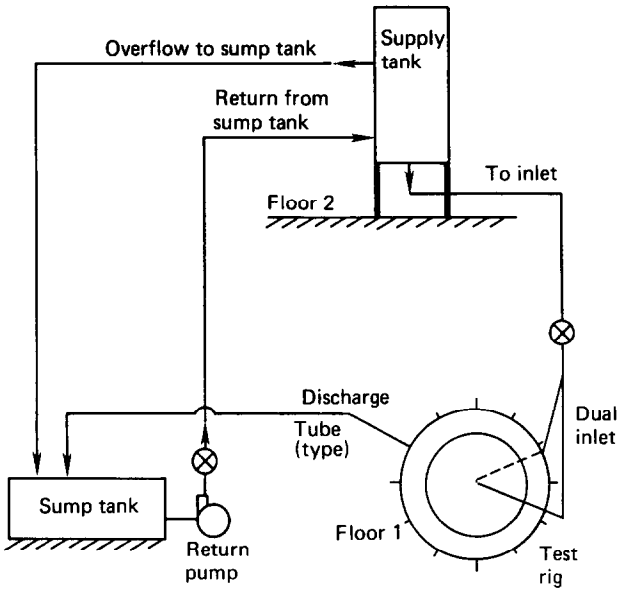

Figure 3 Side view of rig

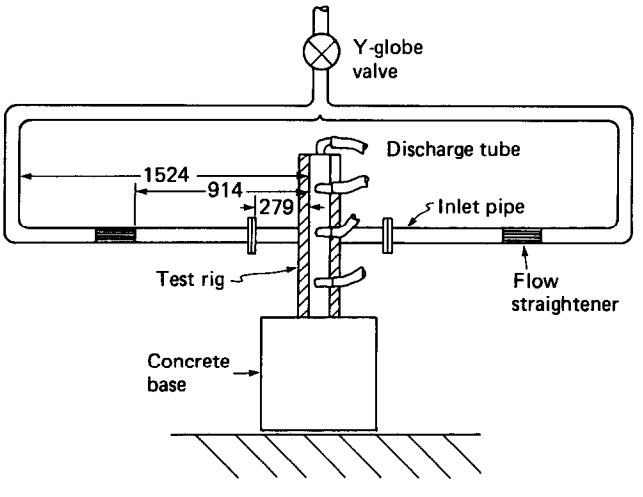

Figure 4 Flow loop

holes were equally spaced aroung the plenum walls to discharge the fluid.

The diffuser model was mounted vertically on a 0.6 m × 0.6 m × 1.2 m concrete base. Between the floor and the base resided a neoprene vibration damping pad.

The test loop

Water was supplied to the diffuser model from a constant-level 3.0 m^3 gallon tank stationed 10 m above the apparatus. The position of the supply tank relative to the diffuser, and other details of the test loop, are depicted in Fig 3. Water flowed out the bottom of the supply tank through 76 mm ABS pipe to the test rig. Flow rate was measured with an orifice meter and was controlled by a Y-globe valve. The valve was positioned immediately before the flow split into the two lines that supplied the diffuser. A straight section of piping (1.5 m) lead to each side of the diffuser. Fig 4 shows these supply lines and their dimensions. A flow straightener was located in each line leading into the diffuser.

From the model the water was carried through the twelve equal length, flexible discharge tubes which lead to a long tank. Return flow was accomplished with two centrifugal pumps positioned in parallel to provide return flow to the supply tank. A constant level was maintained in the tank with an overflow line that lead directly from the supply tank water level to the sump tank.

Flow visualization techniques

In order to determine the qualitative flow behaviour in the diffuser, tufts were used for simple flow visualization. A field of tufts was placed over the lower half of the test area with increased densities in the blade passages near suspected regions of flow separation. The tuft material was the tip of a black marabou plume (13 mm long). All of the tufts were positioned parallel to anticipated streamlines, with the free end downstream of the attached end.

Tufts do not provide any information other than the direction of the flow, although they do have the advantage of making a flow pattern near the wall immediately obvious. For the case of the vaneless diffuser the angle of the flow was the most critical parameter; thus the tufts were ideally suited to the purpose. With blades installed, the flow angle was of equal importance to the size and shape of the separation regions. To assist with the identification of these regions, dye was injected into the area through the specially located dye injection holes. The dye used was a neutral buoyancy mixture of water-soluble black ink and pure ethyl alcohol. Both the tuft behaviour and the dye injection patterns were recorded on photographic film via a 35 mm camera.

Test procedure

The diffuser was assembled with the tufts and the desired number of blades in place. Once the diffuser was started, the Y-globe valve was adjusted to provide the required flow rate.

All of the tests were run at 6.31 litre/s, which corresponds to a Reynolds number based on the absolute fluid velocity and axial passage thickness of 24 400 at the blade tip. The velocity at the leading blade tip was 2.15 m/s.

After the diffuser was steadily operating, a number of photographs were taken of the tufts under the influence of the flow. For the four-, six- and eight-vaned diffuser configurations ink was also injected into each of the separation regions and allowed to saturate the separated area before the photographs were taken. Approximately six photographs were taken of each blade. Although the separation region did fluctuate slightly with time, the actual separation point did not.

Results

The intent of this research was to document the flow behaviour in the diffuser using large-scale flow visualization. Results are presented and discussed in this section.

Vaneless diffuser

Photographs were first taken of the tufts under the influence of the flow with no blades installed. To analyse these photographs the diffuser was divided into ten equal radial zones with the swirl

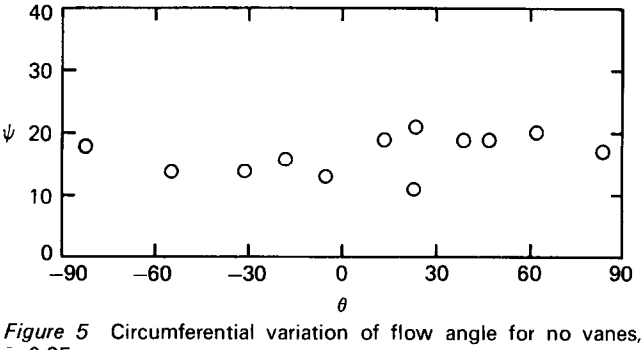

Figure 5 Circumferential variation of flow angle for no vanes, $\bar{r}$=0.35

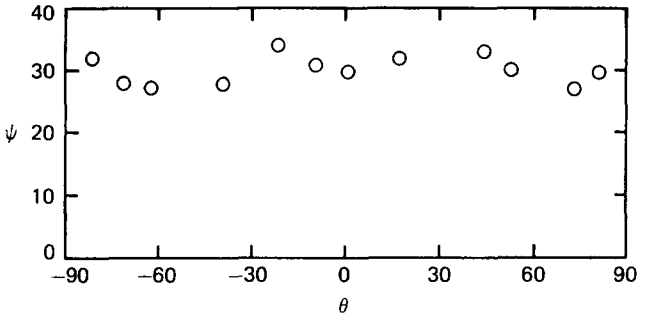

Figure 6 Circumferential variation of flow angle for no vanes, $r=0.55$

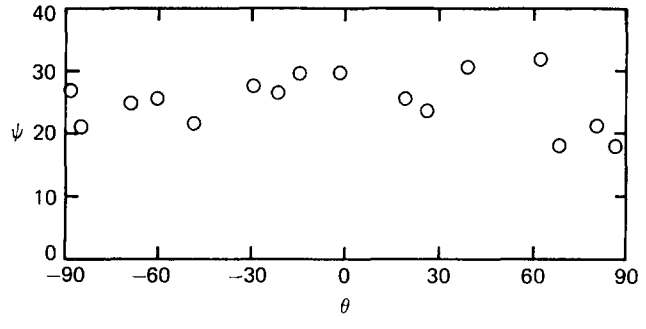

Figure 7 Circumferential variation of flow angle for no vanes, $r=0.75$

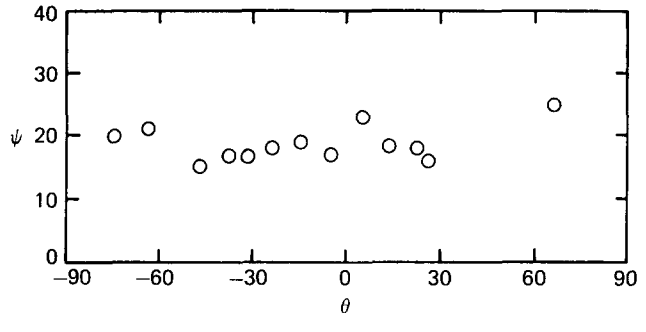

Figure 8 Circumferential variation of flow angle for no vanes, $r=0.95$

generator occupying the first three zones. Figs 5–8 are typical plots of the flow angle of each tuft within a radial zone plotted against its angular location within the zone. The flow angles nearest the swirl generator ($\bar{r}=0.35$) and those nearest the outer baffle vanes ($\bar{r}=0.95$) show maximum scatter of 12° and sample standard deviation of 2.6°. At $\bar{r}=0.75$ the maximum scatter is 14° with a sample standard deviation of 4.4°. The scatter in these data is attributed to two effects. First, the inlet swirler was imparting some small circumferential deviations at the inlet as a result of manufacturing tolerances. Second, because the slots on the side walls were filled with caulk some small roughness effects altered the flow slightly.

In Fig 9 the mass averaged value of the flow angles for each radial zone are plotted against the mean radius of the zone. Also included in this figure are four- and eight-vaned cases which are discussed below. As $\bar{r}$ increases, the flow-angle rises from 16° to a peak of 27.5° at $\bar{r}=0.55$ and then returns to 16° at $\bar{r}=0.95$. As is discussed in Ref 10, this trend is a result of viscous forces and is expected.

Four-vaned diffuser

As was done for the vaneless diffuser, a photograph of the tufts was divided into ten radial zones for analysis. Only those tufts outside of the observed separation regions were analysed.

Fig 9 shows the mean flow angle versus the mean dimensionless radius of the data zone. Also shown in Fig 9 are the radial positions of the blade leading and trailing edges. Because of the separation regions, large variations in the radial distribution of the flow angle from the vaneless diffuser were found. One can see that the flow angles in the vane region are approximately 10°, approximately 15° below the vaneless diffuser case. The presence of the four blades did not strongly affect the flow angle in the inner vaneless region ($\bar{r}\leqslant 0.50$); the angle remained close to 16°. Beyond the blades the flow angle increased to 27° ($\bar{r}=0.75$) and then rapidly decreased to 14.5° near the outlet ($\bar{r}=0.95$). This rapid reduction was due to the baffle vanes located at the exit.

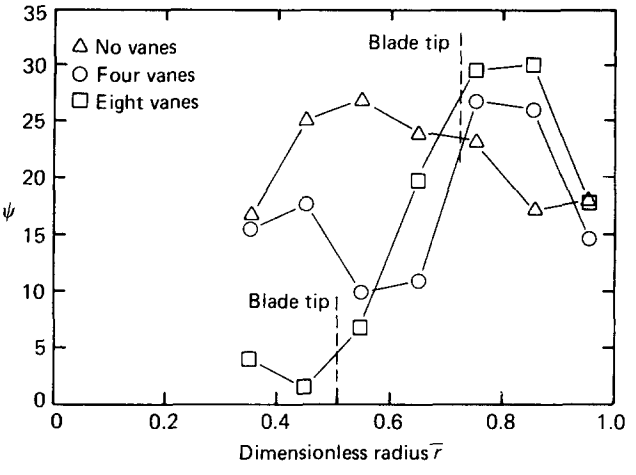

Figure 9 Radial variation of average flow angle

Figure 10 Typical dye injection photograph (blade No. 1) showing separation for four blades

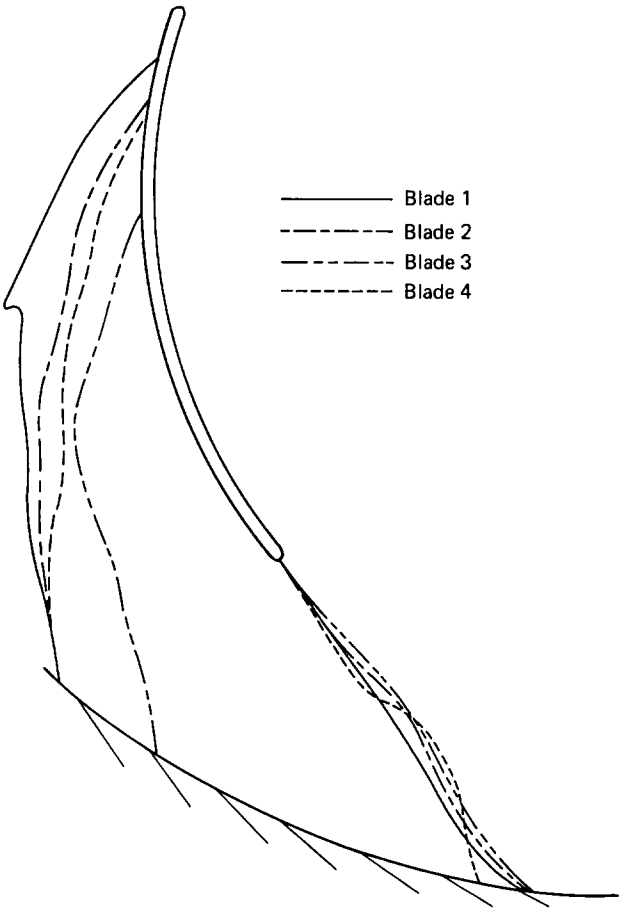

Figure 11 Composite of separation zone—four blades

The small flow angle within the blade region was neither expected nor predicted[10]. One possible explanation for this behaviour is that the separation zone and boundary layers on the blade surfaces and side walls are interacting, which induces secondary flows. Since the tufts are on the side walls, they will indicate the direction of a combination of through-flow and secondary flow velocities. The tufts along the leading length of the blades showed an angle that was not parallel to either the vane or the separation area unless they were adjacent to these surfaces. This observation substantiates the secondary flow postulation.

A typical photograph with dye injection is shown in Fig 10 for blade number 1. As can be seen, a large separation zone occurs. Also, the tufts near this blade are evident.

Fig 11 is a composite diagram of the separation areas on the four blades. The onset of separation varies between 9% and 33% of the blade length from the blade leading tip, with an average value of 23%. The authors of Ref 10 predicted the separation point to occur at 20% of the blade length also on the convex side of the blade. The small difference between predicted and observed separation points is attributed to the fact that the predictions are for 2-D flow, whereas the experimental flow was 3-D as a result of the side wall boundary layers. The differences on the separation zones are probably due to the fact that the flow angles on the vaneless diffuser were not circumferentially constant. In Fig 12 the average separation regions are combined so as to yield an overall indication of the flow patterns. As can be seen, despite the early onset of separation, the separation zones are not blocking the flow passages.

In Fig 13 the percentage of blockage of a diffusing passage, based on the average separation size, is plotted versus the range of radii. The blockage indicates how much area was available for radial flow. At the largest blockage ($\bar{r}=0.85$), the separation region blocked 38% of the passage area.

Six-vaned diffuser

Results for the six-bladed diffuser fall between those for the four- and eight-vaned cases. These results are not discussed in detail, but summarized results are presented in Figs 14 and 15.

Basically, the average separation began at 27% of the blade length from the leading edge. Thus, the additional blades

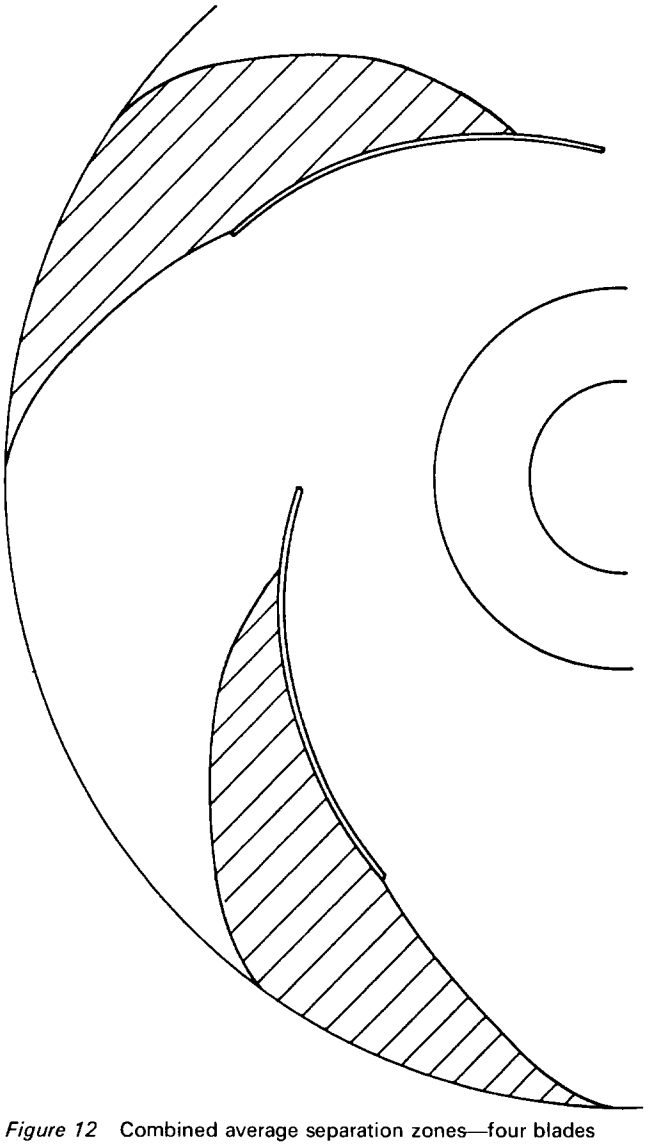

Figure 12 Combined average separation zones—four blades

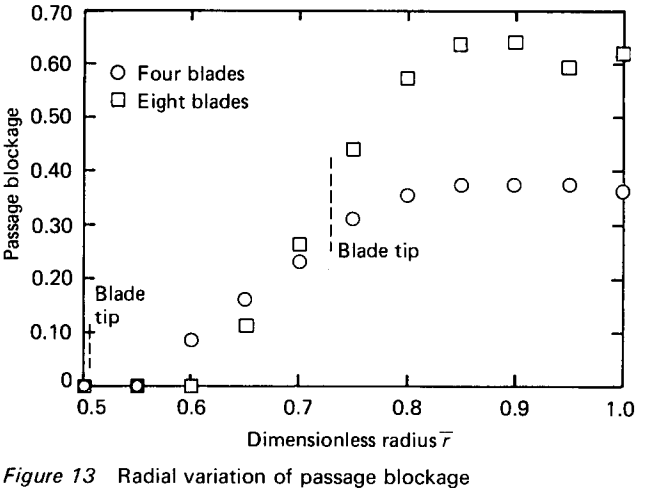

Figure 13 Radial variation of passage blockage

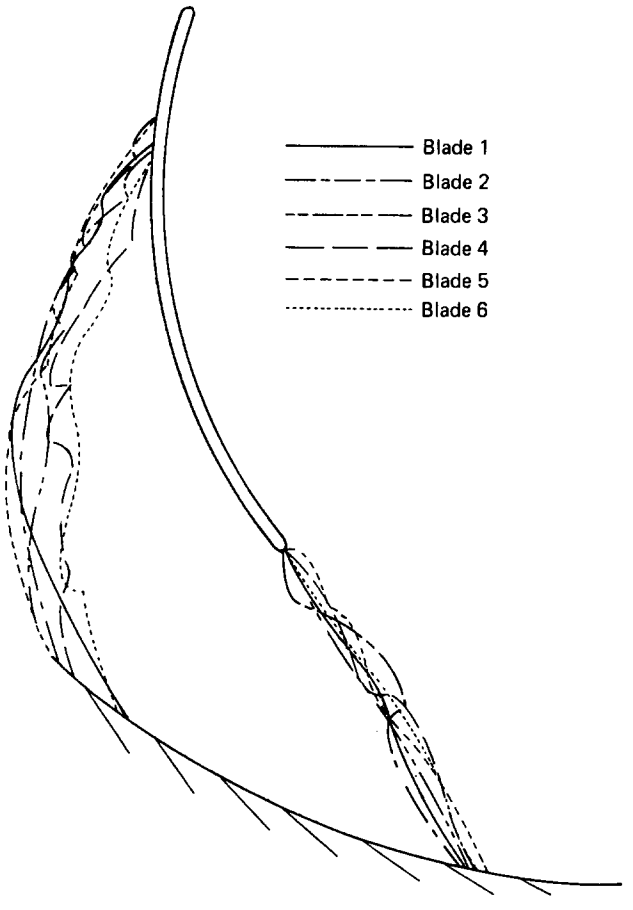

Figure 14 Composite of separation zones—six blades

delayed separation slightly. The shape of the separated region is similar to the four-bladed case.

Eight-vaned diffuser

The plot of mean flow angle versus mean zone dimensionless radius for the eight-blade configuration is also shown in Fig 9. The trend of the flow angle with increasing radius is similar for eight and four blades. For eight blades the measured flow angle in the inner vaneless region ($\bar{r}=0.35$) was reduced to 4°. Again, boundary layer interactions or secondary flows probably caused this reduction. Photographs showed that the tufts indicated angles not parallel to the blades unless they were adjacent to the blades. As the separation region grew, the flow angle increased in the radial direction. The influence of the baffle vanes can be seen because the flow angle drops sharply to 18° at $\bar{r}=0.95$.

Fig 16 is a composite drawing of the separation regions and Fig 17 shows the average separation zones. The onset of separation occurred between 38% and 58% of the blade length from the blade tip, with an average at 50%. In Ref 10 this separation point was predicted to occur at 43% of the blade length. Again, the difference between predicted and measured separation points is attributed to the fact that the analysis is 2-D in nature. Thus the additional blades significantly delayed separation compared with the previous two cases. In general the individual eight-blade separation regions were smaller than the four-blade regions. Despite their smaller size, however, the eight separation regions combined to constrict more significantly the blade passages, as is evident in Figs 13 and 17. At the peak development of the separation region ($\bar{r}=0.9$) 64% of the area was blocked, compared with a maximum of 38% for the four-bladed case.

Summary

A clear plastic model of a vaned diffuser was constructed and large-scale flow visualization tests using tufts and dye injection were conducted. The objective was to document the model's flow behaviour with zero, four, six, and eight blades installed. The average Reynolds number was 20000. A summary of the main findings follows.

(1) As a vaneless diffuser, the flow angle radially varied as much as 11° from the ideal 16°. This variation is caused by the viscous effects.
(2) With four blades installed, separation began at 23% of the blade length from the leading edge and on the convex side of the blade. The effect of separation was to reduce the flow angle at inner radii and to increase the flow angle at outer radii. Predictions indicated that the separation should begin at 20% from the leading edge.
(3) With six blades, separation began at 27% of the blade length from the tip.
(4) With eight blades installed, separation began at 50% of the blade length from the blade tip. The reduction of inner radii flow angles and increase of outer radii flow angles were very pronounced. Predictions indicated that the separation should begin at 43% from the leading edge.
(5) The four-vaned diffuser experienced a maximum blockage of 34% of the total passage area, while the eight-vaned

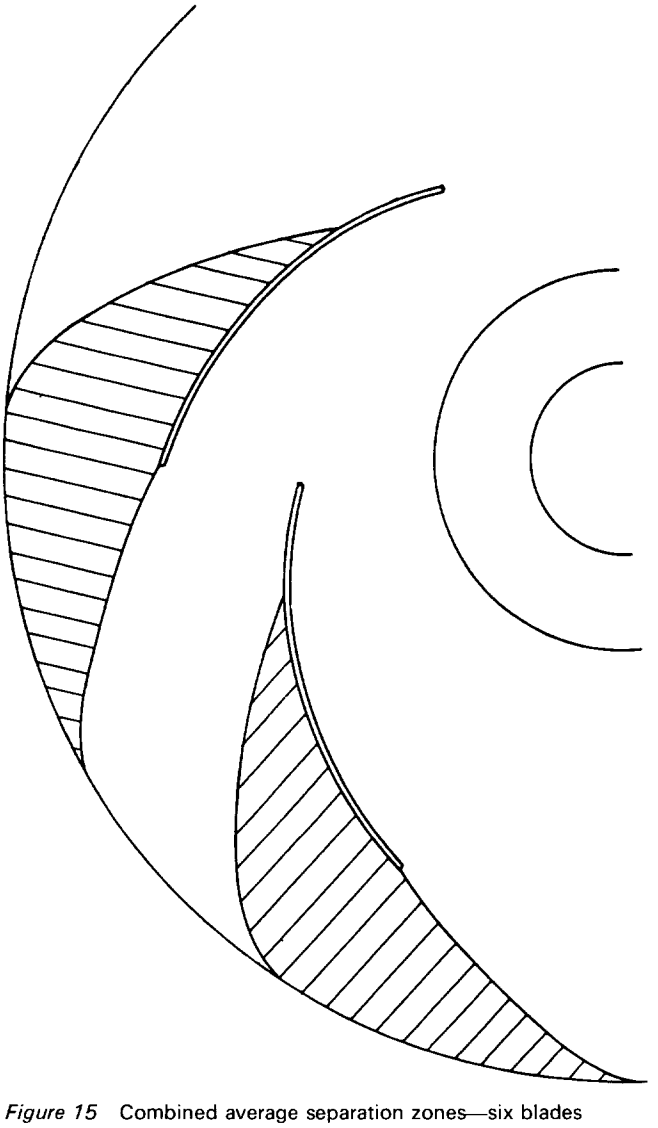

Figure 15 Combined average separation zones—six blades

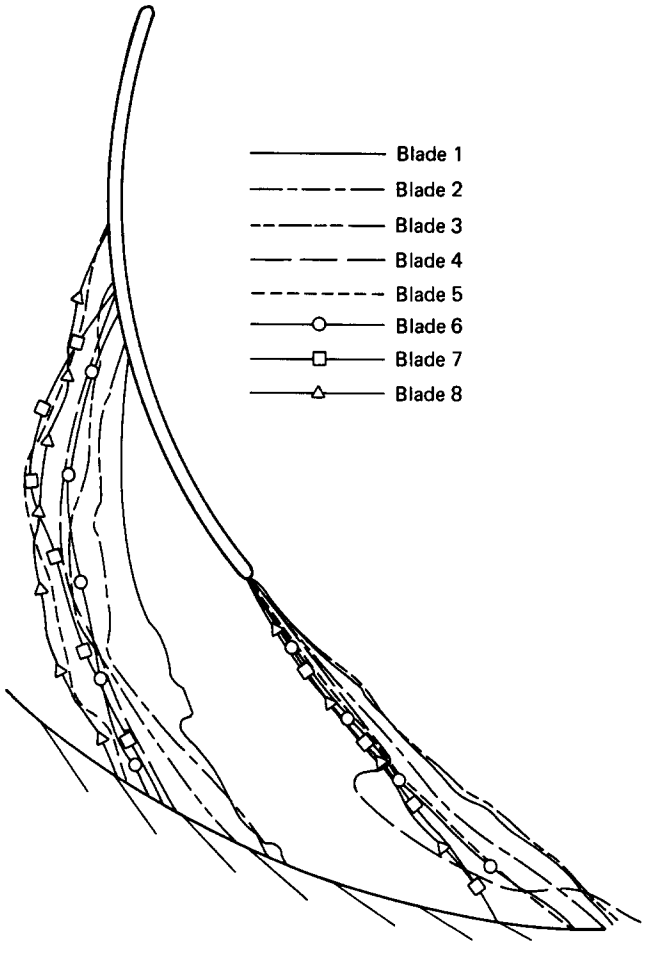

Figure 16 Composite of separation zones—eight blades

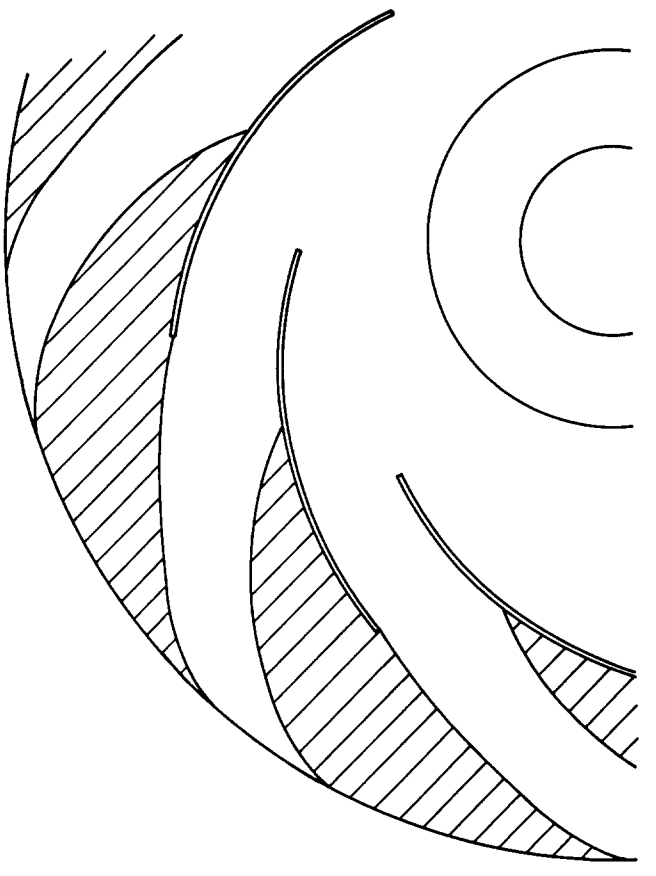

Figure 17 Combined average separation zones—eight blades

diffuser experienced a maximum blockage of 64% of the total passage area.

(6) The current qualitative results will be used as guides for future LV measurements in the same rigs to quantitatively evaluate the diffuser performance.

Acknowledgement

This work was sponsored by the Rotating Machinery and Controls (ROMAC) Industrial Research Program at the University of Virginia.

References

1 Brownell, R. B. and Flack, R. D. Flow characteristics in the volute and tongue region of a centrifugal pump. *ASME Paper* 84-GT-82

2 Pampreen, R. C. The use of cascade technology in centrifugal compressor vaned diffuser design. *J. Eng. for Power, Trans ASME*, July 1972, **94**(3), 187–192

3 Sakurai, T. Flow separation and performance of decelerating channels for centrifugal turbomachines, *J. Eng. for Power, Trans. ASME*, July 1975, **97**(3), 388–394

4 Baghdadi, S. The effect of rotor blade wakes on centrifugal compressor diffuser performance — a comparative experiment. *J. Fluids Eng. Trans. ASME*, March 1977, **99**(1), 45–52

5 Yoshinaga, Y., Gyobu, I., Mishina, H., Koseki, F. and Nishida, H. Aerodynamic performance of a centrifugal compressor with vaned diffusers. *J. Fluids Eng. Trans. ASME*, December 1980, **102**(4), 486–493

6 Krain, H. A study of centrifugal impeller and diffuser flow. *J. Eng. for Power, Trans. ASME*, October 1981, **103**(4), 688–697

7 Senoo, Y., Hayami, H. and Ueki, H. Low-solidity tandem-cascade diffusers for wide-flow-range centrifugal blowers. *ASME Paper* 83-GT-3

8 Bammert, K., Jansen, M. and Rautenberg, M. On the influence of the diffuser inlet shape on the performance of a centrifugal stage. *ASME Paper* 83-GT-9

9 Stein, W. and Rautenberg, M. Flow measurements in two cascaded vane diffusers with different passage widths. *ASME Paper* 85-GT-46

10 Schnipke, R. J., Rice, J. G. and Flack, R. D. Finite element analysis of the viscous flow in a vaned radial diffuser. Concurrently submitted to *Int. J. Heat and Fluid Flow*